Article

Interrogating Signaling Nodes Involved in Cellular Transformations Using Kinase Activity Probes

Cliff I. Stains,[1,4] Nathan C. Tedford,[2] Traci C. Walkup,[3] Elvedin Luković,[1] Brenda N. Goguen,[1] Linda G. Griffith,[2] Douglas A. Lauffenburger,[2] and Barbara Imperiali[1,3,*]

[1]Department of Chemistry
[2]Department of Biological Engineering
[3]Department of Biology
Massachusetts Institute of Technology, Cambridge, MA, 02139, USA
[4]Present address: Department of Chemistry, University of Nebraska-Lincoln, Lincoln, NE 68588, USA
*Correspondence: imper@mit.edu
DOI 10.1016/j.chembiol.2011.11.012

SUMMARY

Protein kinases catalyze protein phosphorylation and thereby control the flow of information through signaling cascades. Currently available methods for concomitant assessment of the enzymatic activities of multiple kinases in complex biological samples rely on indirect proxies for enzymatic activity, such as posttranslational modifications to protein kinases. Our laboratories have recently described a method for directly quantifying the enzymatic activity of kinases in unfractionated cell lysates using substrates containing a phosphorylation-sensitive unnatural amino acid termed CSox, which can be monitored using fluorescence. Here, we demonstrate the utility of this method using a probe set encompassing p38α, MK2, ERK1/2, Akt, and PKA. This panel of chemosensors provides activity measurements of individual kinases in a model of skeletal muscle differentiation and can be readily used to generate individualized kinase activity profiles for tissue samples from clinical cancer patients.

INTRODUCTION

Current techniques for analyzing the signaling dynamics of multiple protein kinases in complex samples use proxies for kinase activity, such as antibody- or mass spectrometry-based analysis of phosphorylation states (Choudhary and Mann, 2010; Nielsen et al., 2003; O'Neill et al., 2006; Xiao et al., 2010). In one embodiment of this approach, the activities of target kinases are inferred through analysis of the phosphorylation state of specific substrates. For example, activation of PKA is often demonstrated through the phosphorylation of its downstream substrate CREB (Chen et al., 2005; Gonzalez and Montminy, 1989). These inferences of enzymatic activity generally lack a temporal component, making the interpretation of enzymatic rates difficult. In a complementary approach, the activation of particular kinases is inferred through the phosphorylation state of those kinases. Coupling this antibody-based approach with

isoelectric focusing allows for quantitative measurement of the phosphorylation status of a kinase (O'Neill et al., 2006). However, measurements of activating phosphorylation modifications on an individual kinase are inherently univariate and do not take into account other cellular processes, such as additional posttranslational modifications that may affect kinase activity (Chen et al., 2001). Indeed, activating phosphorylation modifications of a particular kinase do not always correlate with its enzymatic activity (Kumar et al., 2007). This has prompted a shift away from analysis of proxies for kinase activation toward the development of sensors capable of reporting directly on the enzymatic activity of a particular kinase. Notably, FRET-based sensors, incorporating genetically encodable fluorescent proteins, have been used to detect kinase activity in living cells (Kunkel et al., 2007; Sato et al., 2007). However, these probes often only produce modest increases in fluorescence of ~20%–60% upon phosphorylation (Rothman et al., 2005), and their application in tissues isolated from clinical patients has not been demonstrated. Recently, the Lawrence laboratory observed that tyrosine phosphorylation alleviates quenching of a proximal fluorophore (Wang et al., 2006). This phenomenon was utilized to generate orthogonal activity probes capable of monitoring two tyrosine kinase activities simultaneously (Wang et al., 2010). Although elegant, this strategy is currently restricted to tyrosine kinases and does not allow for analysis of serine/threonine kinase activities, which constitute important downstream signaling nodes within cellular pathways.

In order to address these issues, our laboratories developed a technique in which a phosphorylation-sensitive fluorescent amino acid, Sox, is used to monitor kinase activity in unfractionated cell lysates (Shults et al., 2005). Phosphorylation at a proximal residue dramatically increases the affinity of Sox for Mg^{2+}, leading to an increase in fluorescence, a process termed chelation-enhanced fluorescence (Shults and Imperiali, 2003). This sensing modality is general and can be applied to substrates for both tyrosine and serine/threonine kinases. Recently, we have extended this strategy through the development of a second-generation cysteine derivative of the Sox fluorophore, which we term CSox (Luković et al., 2008) (Figures 1A and 1B). The increased flexibility of CSox allows for incorporation of both N- and C-terminal kinase recognition elements into second-generation probes, leading to improved selectivity and kinetic properties as well as lower sample demand. We have
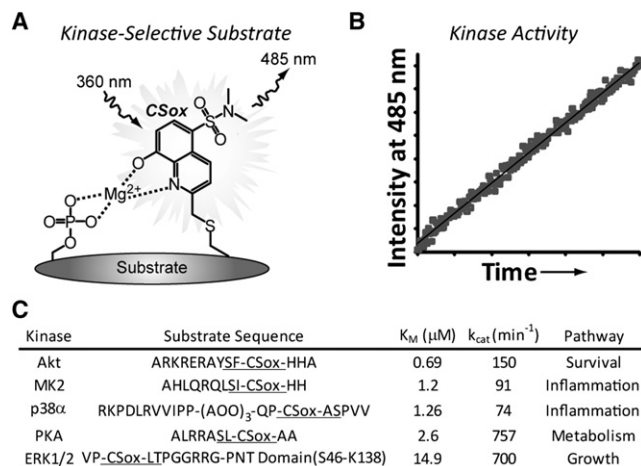
Figure 1. CSox-Based Kinase Activity Probes

(A) Phosphorylation of a kinase substrate containing CSox leads to chelation of Mg^{2+} and an increase in CSox fluorescence.

(B) Phosphorylation can be directly monitored in unfractionated lysates by exciting at 360 nm and measuring emission at 485 nm. The rate of increase in fluorescence is proportional to enzymatic activity.

(C) A panel of selective kinase activity sensors with corresponding kinetic parameters is shown (Luković et al., 2008, 2009; Stains et al., 2011). The CSox amino acid and sites of phosphorylation are underlined. The p38α sensor contains a flexible 8-amino-3,6-dioxaoctanoic acid (AOO) linker between a p38α peptide-based docking sequence and phosphorylation site (Stains et al., 2011), whereas the CSox phosphorylation site of the ERK1/2 sensor is ligated to a protein docking domain for ERK1/2 (Luković et al., 2009). Canonical pathways for each kinase are indicated.

See also Figure S1.

Figure 2. Longitudinal Kinase Activity Dynamics During Differentiation of C2C12 Cells

A hierarchal clustering analysis of fold changes in kinase activity relative to cells grown under mitogen-rich conditions demonstrates clustering of kinases based on similar trends in activity.

See also Figure S2 and Movie S1.

previously developed CSox-based sensors for p38α, ERK1/2, MK2, Akt, and PKA (Luković et al., 2008; Luković et al., 2009; Shults et al., 2005; Stains et al., 2011) and have derived kinetic parameters for each substrate (Figure 1C). The selectivity of the p38α and ERK1/2 sensors has been verified using a panel of recombinant kinases with potential overlapping substrate specificity as well as unfractionated cell lysates in combination with inhibitors and immunodepletions (Luković et al., 2009; Stains et al., 2011). In a similar manner, the selectivity of second-generation CSox sensors for MK2, Akt, and PKA (Luković et al., 2008) were evaluated in unfractionated cell lysates through the use of inhibitor assays and immunodepletions, demonstrating that these sensors are also selective for the targeted kinase (Figure S1 available online). Importantly, the improved catalytic efficiency of the MK2 and Akt second-generation sensors (Luković et al., 2008) (10- and 23-fold respectively), compared with our previous design (Shults et al., 2005), allows for decreased sample and substrate demand while maintaining assay performance. In addition, off-target kinase inhibitors may be removed from the MK2 assay while maintaining selectivity (Figure S1).

The above panel of selective kinase activity sensors has the potential to provide information concerning signaling flux through biologically important pathways that impinge upon cell survival, growth, metabolism, and inflammatory responses (Figure 1C). To demonstrate the utility of this panel, we used it two different ways—namely, longitudinally and latitudinally. In the
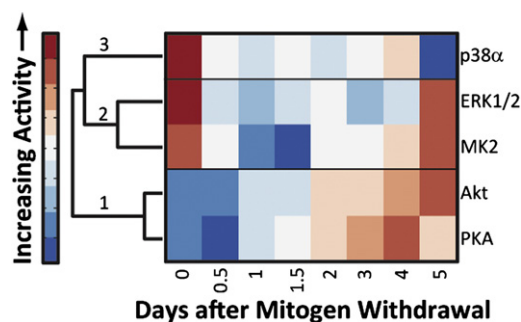
first, we delineate perturbations in multipathway signaling network activities during skeletal muscle differentiation; in the second, we compare multipathway signaling network activities between diseased and normal tissue in individual human tumors, potentially clarifying previously ambiguous roles for kinases within the panel. These experiments highlight the utility of direct activity measurements in providing unique information concerning operative signaling pathways.

RESULTS AND DISCUSSION

A Longitudinal Analysis of Kinase Activity during Skeletal Muscle Differentiation

We began with a study aimed to determine how multiple kinase activities might vary during a time course of cellular differentiation. We selected skeletal muscle differentiation as an important example application and implemented the well-studied C2C12 mouse myoblast cell line. These mononucleated progenitor cells can be induced to exit the cell cycle and differentiate into fused multinucleated myotubes upon mitogen withdrawal (Figure S2) and display characteristic phenotypic changes such as spontaneous contraction (Movie S1). C2C12 lysates were prepared after mitogen withdrawal over a 5-day period, and, in addition to the phenotypic changes noted above, differentiation was confirmed by monitoring the expression of early and late stage markers (Figure S2).

Having established the phenotypic differentiation process, we determined the activity of each kinase in the panel relative to myoblasts grown under mitogen-rich conditions for two independent preparations of cell lysates (Figure S2). Relative changes in kinase activity were used in hierarchical clustering analysis to identify activities which correlate with differentiation (Figure 2). This analysis identified three clusters that showed distinct activity profiles. Cluster 1 contained PKA and Akt activities, which were positively correlated with differentiation (Figure 3A). In addition, western blot analysis of phospho-Akt levels correlated well with the direct Akt activity assays and indicated that the increase in observed Akt activity may be due to an increase in Akt expression (Figure 3A, inset). These data support previous observations indicating that both PKA and Akt are
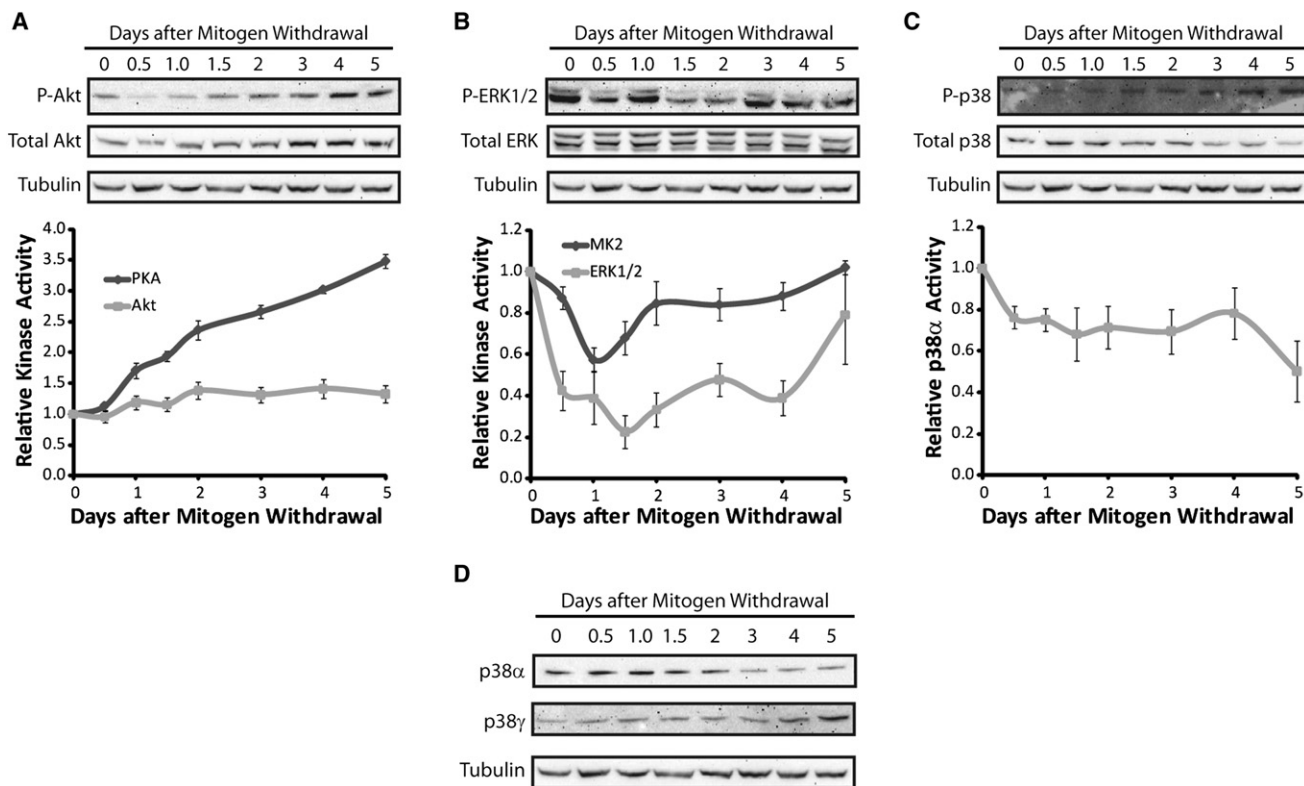
Figure 3. Relative Activity Trends of Kinases during Differentiation of C2C12 Cells
(A–C) Fold changes in activity for clusters 1, 2, and 3, respectively. Activity assays demonstrate linkages between pathways that are operative during differentiation, and insets within each panel show western blots for the corresponding phosphokinase with tubulin as a loading control. Relative changes in activity are the average of six total activity assays performed on two independently prepared C2C12 cell lysates ± SEM.
(D) Western blot analysis of p38α and γ expression during C2C12 differentiation. Tubulin serves as a loading control.
See also Figure S2 and Movie S1.

positive regulators of myogenesis (Chen et al., 2005; Fujio et al., 1999; Mukai and Hashimoto, 2008; Rommel et al., 1999). Cluster 2 activity, which includes ERK1/2 and MK2, displayed a biphasic activity profile (Figure 3B). Biphasic ERK1/2 activity has been previously observed using western blot analysis and did not correlate with ERK expression (Figure 3B, inset). This ERK activity profile is thought to facilitate exit from the cell cycle (Rommel et al., 1999; Tagawa et al., 2008). Interestingly, MK2 activity displays a similar activity profile, which is in agreement with previous studies that have observed a linkage between MK2 and ERK1/2 signaling (Aldridge et al., 2009; Coxon et al., 2003), which may also operate during myogenesis. Finally, p38α activity decreased marginally during the time course studied (Figure 3C) and appeared to be negatively correlated with phopho-p38 levels while being positively correlated with total p38 expression, as observed by western blotting (Figure 3C, inset). Importantly, currently available phospho-p38 antibodies do not distinguish between p38 isoforms (α, β, γ, and δ). Indeed, our observed pattern of p38α activity agrees with assays performed on kinase immunoprecipitated with antibodies that specifically recognize this isoform, regardless of phosphorylation status (Perdiguero et al., 2007). The inability to resolve p38 isoform activation with currently available antibodies has lead to the use of mice expressing reduced amounts of each p38 isoform (α, β, γ, and δ)

or RNA interference to identify essential p38 isoforms for myogenesis (Perdiguero et al., 2007; Wang et al., 2008). However, these relatively complex genetic analyses have been unable to identify the p38 isoform observed using phosphospecific antibodies. Our data suggest that the observed increases in the phosphorylation state of p38 are not due to p38α, but are likely due to an alternate isoform. Interestingly, p38γ transcript (Tomczak et al., 2004) and protein levels (Wang et al., 2008) (Figure 3D) increase dramatically following mitogen withdrawal in C2C12 cells, and overexpression of this p38 isoform has previously been shown to stimulate C2C12 differentiation (Lechner et al., 1996). Previous studies have demonstrated that p38δ is not expressed in C2C12 cells and that p38β expression decreases dramatically during differentiation in contrast to p38α, which is expressed throughout the myogenic program (Wang et al., 2008) (Figure 3D). Furthermore, in vitro activity assays using immunoprecipitated kinase have demonstrated an increase in p38γ activity during myogenesis (Perdiguero et al., 2007). Taken together, these observations could account for the observed increase in the amount of an unidentified phosphorylated p38 isoform (Perdiguero et al., 2007). In this light, our observations support distinct roles for more than one p38 isoform during myogenesis (Wang et al., 2008) and are consistent with previous observations that indicate an essential role for p38α (Perdiguero
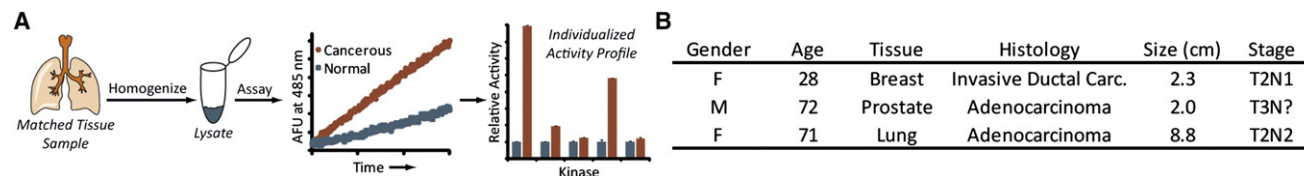
Figure 4. Kinase Activity Profiling in Human Tumors
(A) A workflow diagram for analysis of matched tissues using CSox-based kinase activity sensors.
(B) Clinical and histological features of cancer patients.
See also Figure S3.

et al., 2007), because signaling dynamics with durations less than 12 hr are not resolved in this experiment. These activity measurements underscore the utility of direct activity sensors for determining operative signaling networks during cell differentiation.

A Latitudinal Analysis of Alterations in Kinase Signaling in Individual Human Tumors

To examine the capability for ascertaining modulations in multiple kinase enzymatic activities between normal and diseased tissue samples, we selected the problem of comparing matched tissues from cancer patients in three different pathology contexts (Figure 4A). In particular, our panel of activity probes contains kinases that may have prognostic value and have been implicated in the development of breast, prostate, and lung cancers (Feldman and Feldman, 2001; Gustafson et al., 2010; Musgrove and Sutherland, 2009). Accordingly, we obtained matched tumor and healthy control tissues from patients diagnosed with these diseases (Figure 4B) and set out to construct individualized kinase activity profiles for each.

Lysates were prepared from each tissue and normalized to total protein content, which was verified through analysis of β-actin levels (Figure S3). In order to demonstrate the robust reproducibility of the observed changes, assays were performed in triplicate on three independently prepared sets of lysates from each pair of matched tissues (Figure S3) and were averaged to obtain individualized patient activity profiles (Figures 5A–5C). The ease of sample preparation, rapid analysis time (<1 hr), and simple instrumentation used for data acquisition make this method practical for potential applications in diagnostic analyses. Moreover, triplicate assays for the entire sensor panel in 96-well format necessitated only 34 mg of tissue, because typical lysate total protein yields were ≥ 3 mg/ml. Assays could also be translated to 384-well plate format (Figure S3), generating equivalent signal-to-noise while using 4-fold less reagents and lysate. These activity measurements reflect the specific biochemistry of individual tumors and could therefore find utility in both assessing disease state and determining effective treatment strategies (Feldman and Feldman, 2001; Gustafson et al., 2010; Musgrove and Sutherland, 2009). Indeed in our limited sample set, we find individual activity profiles that point to (1) the possible benefit of combining tamoxifen with ERK inhibitors for the treatment of an individual breast cancer tumor (Musgrove and Sutherland, 2009) (Figure 5A), (2) increased activity of a potential marker for aggressive prostate cancer (Pollack et al., 2009) (Figure 5B), and (3) aberrant activation of p38α and Akt in a lung cancer tumor (Greenberg et al., 2002; Gustafson et al., 2010) (Figure 5C). The implications of these unique activity profiles are discussed in further detail below.

In the breast tumor samples, clear enhancements in p38α (3.2 ± 0.34-fold), MK2 (2.7 ± 0.11-fold), and ERK1/2 (2.7 ± 0.15-fold) activities were observed relative to surrounding normal tissue (Figure 5A). These alterations in activity were supported by western blot analysis (Figure 5A, inset). The expression of estrogen, progesterone, and ErbB2 receptors serves to stratify breast cancer patients and determine clinical treatment strategies (Musgrove and Sutherland, 2009). For example, patients with estrogen receptor-positive tumors are generally treated with tamoxifen; however, women treated with tamoxifen for 5 years still have a 33% recurrence rate after 15 years (Musgrove and Sutherland, 2009). Accordingly, diagnostic methods to predict potential resistance to endocrine therapy are needed. In this context, the observed increase in ERK1/2 activity along with receptor status (Figure 5A) provide potential insights into patient-specific responses to traditional therapy, because this kinase has been linked to the development of tumors that are resistant to endocrine therapy (Musgrove and Sutherland, 2009). Moreover, the current difficulty in classifying tumors according to perturbations in enzyme activity is thought to have contributed to the variable results obtained in clinical trials that attempted to resensitize tamoxifen-resistant tumors through administration of ERK inhibitors (Musgrove and Sutherland, 2009). These results suggest that information from direct kinase activity measurements may be useful for identifying individuals who could benefit from combination therapy.

In the prostate tumor sample analyzed here, only PKA activity was altered when compared to surrounding normal tissue, with an increase in activity of 1.8 ± 0.08-fold (Figure 5B). A variety of mechanisms for progression of prostate cancers toward androgen independence in response to traditional androgen deprivation therapy have been described, including activation of ERK and Akt (Feldman and Feldman, 2001). Unfortunately, tumors that have progressed to androgen independence generally lead to poor clinical outcomes. Consequently, methods capable of identifying individuals at risk for progression to androgen-independent cancers would be helpful in diagnostic applications. These data suggest that this particular tumor may not have progressed to an androgen-independent state as assessed through activation of either the ERK or Akt pathways (Feldman and Feldman, 2001). However, a recent study monitoring 313 patients with prostate cancer suggests that increases in PKA activity correlate with poor clinical outcomes in response to traditional androgen deprivation therapy (Pollack et al., 2009), indicating that quantitative knowledge of PKA activity would be useful for providing information on individual disease status.

In the individual lung cancer tumor, an increase in MK2 (2.0 ± 0.06-fold) and Akt (2.3 ± 0.35-fold) along with comparably more
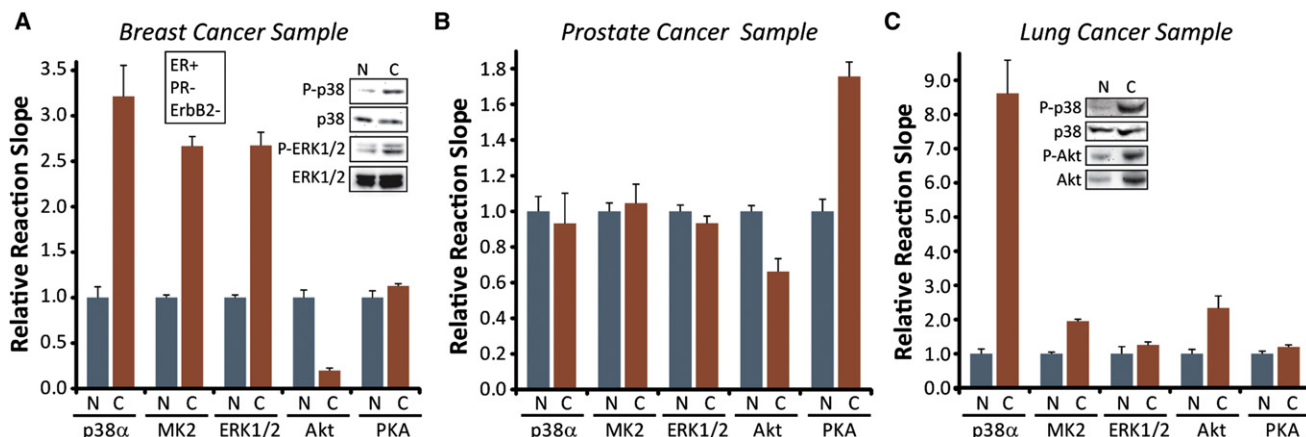
Figure 5. Individualized Kinase Activity Profiles for Clinical Cancer Patients
(A–C) Activities of the indicated kinases in cancerous (C, red) relative to normal (N, blue) breast, prostate and lung tissues, respectively. Distinct changes in kinase activity profiles are observed for each patient and correlate to western blots shown in each inset. The left inset in (A) indicates receptor status for the corresponding tumor. Data represent the average ± SEM of nine total kinase activity assays performed on three independent lysate preparations of each individual set of matched tissues.
See also Figure S3.

dramatic increases in p38α (8.6 ± 0.98-fold) activity was observed (Figure 5C). This aberrant increase in p38α activity was confirmed using western blot analysis and did not appear to be due to an increase in global p38 expression levels, whereas the observed increase in Akt activity correlated with an increase in Akt expression (Figure 5C, inset). Unfortunately, effective treatments for lung cancer, the leading cause of cancer-related deaths, have not been identified. Previous studies have indicated that an increase in Akt activity may be linked to lung cancer progression (Gustafson et al., 2010). The individualized kinase activity profile developed in this study is consistent with these reports, revealing a distinct change (2.4-fold) in Akt activity in normal versus cancerous lung tissue (Figure 5C). Taken together, these data provide corroborating evidence for Akt activation and also confirm p38 as a potential therapeutic target in lung cancer (Greenberg et al., 2002), with p38α contributing substantially to the observed increase in phospho-p38 using western blot analysis (Figure 5C).

Finally, it should be noted that extensive control experiments, including inhibitor assays and immunodepletions (Figure S1) (Luković et al., 2009; Stains et al., 2011), were performed to demonstrate the selectivity of the sensor panel in the presence of endogenous kinases under the described assay conditions. Nonetheless, relatively small contributions from off-target kinases cannot be ruled out in the absence of an exhaustive kinetic analysis of every active human kinase. Consequently, kinase activity alterations are verified through traditional western blotting analysis, highlighting the importance of complementary approaches to measuring kinase activities in complex systems.

SIGNIFICANCE

There is a pressing need for robust technologies to enable direct, quantitative protein kinase activity profiling in basic cell biology, medical diagnostics, and therapeutic agent development. Current methods rely heavily on antibody- or mass spectrometry-based approaches that interrogate pro-

xies for kinase activity. In this article, we demonstrate the power of fluorescence-based kinetic analysis, using the CSox amino acid coupled with kinase-selective substrates, to provide direct measurements of kinase enzymatic activity. Although some residual off-target kinase activity is possible, because the existing panel of sensors has not been assayed against every known human kinase, this limitation is outweighed by the significant advantages of a fluorescence-based kinetic assay. In particular, this study demonstrates that CSox-based probes are capable of providing direct, quantitative readouts of kinase enzymatic activity that clarify the biochemistry of cellular differentiation and individual human tumors. This work provides a proof of principle for expansion to larger sample sizes in order to delineate common perturbations in kinase activities in a given disease. The generality of this sensing strategy also allows for the addition of virtually any kinase of interest to the panel, provided an appropriate substrate sequence can be identified. Currently, our laboratories are working toward expanding the CSox repertoire as well as determining the prognostic value of kinase activity profiling through the study of larger patient populations.

EXPERIMENTAL PROCEDURES

General Reagents

All reagents were of ultrapure, metals-free grade where possible. Buffer 1 is 50 mM Tris-HCl (pH = 7.5 at 25°C), 10 mM MgCl$_2$, 1 mM EGTA, 2 mM DTT, and 0.01% Brij-35-P. Buffer 2 is 50 mM Tris (pH = 7.5 at 25°C), 150 mM NaCl, 50 mM β-glycerophosphate, 10 mM sodium pyrophosphate, 30 mM NaF, 1% Triton X-100, 2 mM EGTA, 100 μM Na$_3$VO$_4$, 1 mM DTT, protease inhibitor cocktail III (10 μl/ml, Calbiochem, 539134), and phosphatase inhibitor cocktail 1 (10 μl/ml, Sigma, P2825).

Synthesis of Kinase Activity Probes

Sensors were synthesized and characterized as described previously (Luković et al., 2008; Luković et al., 2009; Stains et al., 2011). All peptide-based sensors were acetyl-capped at the N terminus and included a C-terminal amide. Concentrations were determined on the basis of the Sox chromophore by

measuring the absorbance at 355 nm in 0.1 M NaOH containing 1 mM Na$_2$EDTA (extinction coefficient = 8427 M^{-1}cm^{-1}) (Luković et al., 2008).

Cell Culture and Lysate Preparation

HepG2 human hepatocarcinoma cells (ATCC, HB-8065) and HT-29 colorectal adenocarcinoma cells (ATCC, HTB-38) were propagated on tissue culture plastic in either Eagle's minimum essential medium (EMEM, ATCC, HepG2) or McCoy's 5a modified medium (ATCC, HT-29) supplemented with 10% FBS (Hyclone, Thermo Scientific) and 1% penicillin/streptomycin (Invitrogen) in a humidified incubator at 37°C and 5% CO$_2$. Prior to stimulation to activate specific kinases, HepG2 cells were plated at 1 × 10^5 cells/cm^2 on collagen-I coated 6-well plates (BD Biocoat, Becton Dickinson) and HT-29 cells were plated at 1 × 10^5 cells/cm^2 on tissue culture treated plastic 6-well plates or 10-cm dishes for inhibitor studies and immmunodepletions, respectively. Both cell types were grown for 24 hr in their respective full medium. Cells were then serum-starved in serum-free medium for 18 hr and dosed with either NaCl (250 mM) for 30 min, insulin (Sigma, I9278, 500 ng/ml) for 5 min, or forskolin (Cell Signaling, 3828, 30 μM) for 15 min. Pretreatment with the upstream kinase inhibitors SB202190 (Calbiochem, 559388), LY294002 (Calbiochem, 440204), or wortmannin (Calbiochem, 681675) was accomplished by adding the indicated molar concentrations to serum-free media 1 hr prior to stimulation. Inhibitor dilutions were prepared such that cells experienced a constant DMSO concentration of 0.1% for all dosing conditions. At the indicated time points, cells were washed with ice-cold PBS and lysed on ice in Buffer 2. Lysates were incubated on ice for 15 min and were clarified by centrifugation. Supernatants were flash frozen in liquid nitrogen and stored at −80°C. These lysates were used to validate second generation CSox-based activity probes for MK2, Akt, and PKA. These experiments demonstrated that less sensor and cell lysate could be used to obtain robust signal-to-noise with the second generation of probes and that inhibitors could be removed from assays for MK2.

HeLa cells were propagated in DMEM (Invitrogen, 11995) supplemented with 10% heat-inactivated FBS and 1% penicillin/streptomycin in a humidified incubator at 37°C and 5% CO$_2$. NIH 3T3 cells were propagated in DMEM supplemented with 10% FBS and 1% penicillin/streptomycin in a humidified incubator at 37°C and 5% CO$_2$. Prior to stimulation cells were starved for 18 hr in DMEM supplemented with 2 mM L-Gln, and 1% penicillin/streptomycin. Sorbitol was then added to a final concentration of 300 mM, and lysates were prepared after 1 hr as indicated above using Buffer 2. C2C12 myoblasts (ATCC, CRL-1772) were propagated in DMEM supplemented with 20% FBS and grown in a humidified incubator with a 10% CO$_2$ atmosphere. Prior to mitogen withdrawal, cells were seeded onto 150-mm collagen-I-coated dishes (BD Biosciences, 354551) at ~40% confluency. At 95% confluency (time 0) cells were switched to DMEM supplemented with 2% horse serum. This medium was replenished daily during differentiation. Lysates were prepared from two separate passages of cells at the indicated time points using the following procedure. Cells were washed with ice-cold PBS and lysed on ice in Buffer 2. Lysates were clarified by centrifugation and supernatants were flash frozen in liquid nitrogen and stored at −80°C. Total protein concentrations for all cell lysates were determined using the BioRad protein assay (500-0006) with BSA as a standard. Lysates were prepared from two separate passages of cells.

Images and videos were acquired using an Olympus IX50 inverted microscope equipped with a 40× phase contrast objective and a QImaging Retiga 2000R camera.

Hierarchical Clustering Analysis

Fold changes in kinase activity were determined relative to time 0 and hierarchical clustering analysis was performed in MATLAB using the built-in Bioinformatics Toolbox with the Euclidean distance metric.

Immunodepletion

HT-29 cells were propagated, plated, starved, stimulated with insulin, and lysed as described above. The flash frozen lysates were thawed on ice and aliquotted in replicates of 500 μg total protein for depleted and control conditions and brought to 100 μl final volume in buffer 2. Lysates were then incubated with either 4 μg of anti-Akt/PKB PH domain 1 antibody (Millipore, 05-591) for Akt immunodepletion or 4 μg of normal mouse IgG (Santa Cruz, sc-2025) as a naive

antibody control for 2 hr at 4°C on a rotator. Samples were then incubated with 40 μl of Protein G sepharose beads (GE Healthcare, 17-0618-01) for 1 hr at 4°C on a rotator. Beads were then pelleted, and supernatants were collected and subjected to two additional rounds of immunodepletion. An input control lysate was aliquoted and kept on ice during all rounds of immunodepletion to account for sample and kinase activity loss during incubation and liquid transfer steps. All lysates were then assayed for Akt kinase activity as described below.

Tissue Lysate Preparation

Tissues were obtained from surgical discards through the National Disease Research Interchange (NDRI) in accordance with an institutional review board-approved protocol from the MIT Committee On the Use of Humans as Experimental Subjects. Tissue samples were flash frozen in liquid nitrogen as soon as possible (~1 hr) after surgery. The guidelines for procurement of snap-frozen tissue may vary slightly because tissues are procured from various surgical sites. Frozen tissues were dissected into ~100 mg sections, placed in a 50 ml conical tube, and washed thoroughly with ice-cold PBS. Lysates were prepared by the addition of 3 volumes (in microliters) of Buffer 2 per mg of tissue and subsequent homogenization on ice with an Omni tissue homogenizer equipped with a plastic homogenizing probe for hard tissues. Samples were then incubated on ice for 1 hr, followed by clarification by centrifugation. The supernatants were collected by piercing the lipid layer and were flash frozen and stored at −80°C. Total protein concentrations were determined using the BioRad protein assay (500-0006) with BSA as the standard.

Cell and Tissue Lysate Assays

Assays were conducted as previously described (Luković et al., 2009; Stains et al., 2011) using the following concentrations of substrates and amounts of lysate for each of the indicated kinases: p38α (1 μM substrate and 10 μg lysate), MK2 (2.5–5 μM substrate and 10–20 μg lysate), ERK1/2 (5 μM substrate and 40 μg lysate), Akt (2.5–5 μM substrate and 10–20 μg lysate), and PKA (10 μM substrate and 20 μg lysate). Inhibitors of off-target kinases were included in assays for p38α (Stains et al., 2011) (1 μM staurosporine), Akt (Shults et al., 2005) (4 μM PKC inhibitor peptide, 4 μM calmidazolium, and 5 μM GF109203X; control experiments demonstrated that addition of PKItide did not influence the rate of phosphorylation of the Akt sensor), and PKA (Shults et al., 2005) (4 μM PKC inhibitor peptide, 4 μM calmidazolium, and 5 μM GF109203X). The activity of p38α was determined by background subtraction in each lysate using 1 μM SB203580 (Stains et al., 2011). Reactions were prepared in Buffer 1 and contained 1 mM ATP, final reaction volumes were 120 μl. Assays were performed in half-area 96-well plates (Corning, 3992), and fluorescence was monitored at 485 nm by exciting at 360 nm using a 455 nm cutoff on a Spectramax Gemini XS plate reader (Molecular Devices) at 30°C. Slopes were determined using linear fits from Excel during the time in which fluorescence increases were linear with respect to time (typically 15–60 min); fits are corrected for lag times in the reaction. Assays with the direct MK2 inhibitor, MK2 Inhibitor III (Calbiochem, 475864), were conducted using NaCl-stimulated HepG2 lysates in presence of the indicated concentration of inhibitor; DMSO concentrations were 1% in the assay. Assays with the direct PKA inhibitors, H89 (Cell Signaling, 9844) and PKItide (Shults et al., 2005), were conducted using forskolin-stimulated HepG2 lysates in the presence of the indicated concentration of inhibitor, in the case of H89 DMSO concentrations were 3% in the assay. The average fold changes for biological replicates of C2C12 lysate and tissue preparations were determined from each individual assay and errors were propagated accordingly.

384-Well Plate Assays

Assays for MK2 activity in 384-well plates (MatriCal, MP101-1-PS) were conducted in a total volume of 30 μl using 5 μM MK2 substrate and 5 μg of lysate; reactions were overlaid with 20 μl of white, light mineral oil prior to recording fluorescence.

Western Blot Analysis

Lysates (20–100 μg total protein) were separated using 12% SDS-PAGE gels, except for myosin heavy chain which was resolved on a 4%–20% gradient gel

(BioRad, 161-1159). Proteins were transferred to a nitrocellulose membrane. Blots were probed with primary antibodies for myogenin (Santa Cruz Biotechnology, sc-12732), myosin heavy chain (R&D Systems, MAB4470), tubulin (Abcam, ab59680), phospho-p38 (Cell Signaling, 9215), total p38 (Cell Signaling, 9212), p38α (Cell Signaling, 9218), p38γ (Cell Signaling, 2307), phospho-ERK1/2 (Cell Signaling, 4377), total ERK1/2 (Millipore, 06-182), phospho-Akt (Cell Signaling, 9271), total Akt (Cell Signaling, 4685), or β-actin (Abcam, ab8227), which were detected using an HRP conjugated goat anti-rabbit (Pierce, 32460) or goat anti-mouse (Pierce, 32430) secondary antibody where appropriate. Blots were visualized by enhanced chemiluminescence (Pierce, 34075).

SUPPLEMENTAL INFORMATION

Supplemental Information includes three figures and one movie and can be found with this article online at doi:10.1016/j.chembiol.2011.11.012.

REFERENCES

Aldridge, B.B., Saez-Rodriguez, J., Muhlich, J.L., Sorger, P.K., and Lauffenburger, D.A. (2009). Fuzzy logic analysis of kinase pathway crosstalk in TNF/EGF/insulin-induced signaling. PLoS Comput. Biol. 5, e1000340.

Chen, A.E., Ginty, D.D., and Fan, C.M. (2005). Protein kinase A signalling via CREB controls myogenesis induced by Wnt proteins. Nature 433, 317–322.

Chen, R., Kim, O., Yang, J., Sato, K., Eisenmann, K.M., McCarthy, J., Chen, H., and Qiu, Y. (2001). Regulation of Akt/PKB activation by tyrosine phosphorylation. J. Biol. Chem. 276, 31858–31862.

Choudhary, C., and Mann, M. (2010). Decoding signalling networks by mass spectrometry-based proteomics. Nat. Rev. Mol. Cell Biol. 11, 427–439.

Coxon, P.Y., Rane, M.J., Uriarte, S., Powell, D.W., Singh, S., Butt, W., Chen, Q.D., and McLeish, K.R. (2003). MAPK-activated protein kinase-2 participates in p38 MAPK-dependent and ERK-dependent functions in human neutrophils. Cell. Signal. 15, 993–1001.

Feldman, B.J., and Feldman, D. (2001). The development of androgen-independent prostate cancer. Nat. Rev. Cancer 1, 34–45.

Fujio, Y., Guo, K., Mano, T., Mitsuuchi, Y., Testa, J.R., and Walsh, K. (1999). Cell cycle withdrawal promotes myogenic induction of Akt, a positive modulator of myocyte survival. Mol. Cell. Biol. 19, 5073–5082.

Gonzalez, G.A., and Montminy, M.R. (1989). Cyclic AMP stimulates somatostatin gene transcription by phosphorylation of CREB at serine 133. Cell 59, 675–680.

Greenberg, A.K., Basu, S., Hu, J., Yie, T.A., Tchou-Wong, K.M., Rom, W.N., and Lee, T.C. (2002). Selective p38 activation in human non-small cell lung cancer. Am. J. Respir. Cell Mol. Biol. 26, 558–564.

Gustafson, A.M., Soldi, R., Anderlind, C., Scholand, M.B., Qian, J., Zhang, X., Cooper, K., Walker, D., McWilliams, A., Liu, G., et al. (2010). Airway PI3K pathway activation is an early and reversible event in lung cancer development. Sci. Trans. Med. 2, 26ra25.

Kumar, N., Afeyan, R., Sheppard, S., Harms, B., and Lauffenburger, D.A. (2007). Quantitative analysis of Akt phosphorylation and activity in response to EGF and insulin treatment. Biochem. Biophys. Res. Commun. 354, 14–20.

Kunkel, M.T., Toker, A., Tsien, R.Y., and Newton, A.C. (2007). Calcium-dependent regulation of protein kinase D revealed by a genetically encoded kinase activity reporter. J. Biol. Chem. 282, 6733–6742.

Lechner, C., Zahalka, M.A., Giot, J.F., Møller, N.P., and Ullrich, A. (1996). ERK6, a mitogen-activated protein kinase involved in C2C12 myoblast differentiation. Proc. Natl. Acad. Sci. USA 93, 4355–4359.

Luković, E., González-Vera, J.A., and Imperiali, B. (2008). Recognition-domain focused chemosensors: versatile and efficient reporters of protein kinase activity. J. Am. Chem. Soc. 130, 12821–12827.

Luković, E., Vogel Taylor, E., and Imperiali, B. (2009). Monitoring protein kinases in cellular media with highly selective chimeric reporters. Angew. Chem. Int. Ed. Engl. 48, 6828–6831.

Mukai, A., and Hashimoto, N. (2008). Localized cyclic AMP-dependent protein kinase activity is required for myogenic cell fusion. Exp. Cell Res. 314, 387–397.

Musgrove, E.A., and Sutherland, R.L. (2009). Biological determinants of endocrine resistance in breast cancer. Nat. Rev. Cancer 9, 631–643.

Nielsen, U.B., Cardone, M.H., Sinskey, A.J., MacBeath, G., and Sorger, P.K. (2003). Profiling receptor tyrosine kinase activation by using Ab microarrays. Proc. Natl. Acad. Sci. USA 100, 9330–9335.

O'Neill, R.A., Bhamidipati, A., Bi, X., Deb-Basu, D., Cahill, L., Ferrante, J., Gentalen, E., Glazer, M., Gossett, J., Hacker, K., et al. (2006). Isoelectric focusing technology quantifies protein signaling in 25 cells. Proc. Natl. Acad. Sci. USA 103, 16153–16158.

Perdiguero, E., Ruiz-Bonilla, V., Gresh, L., Hui, L., Ballestar, E., Sousa-Victor, P., Baeza-Raja, B., Jardí, M., Bosch-Comas, A., Esteller, M., et al. (2007). Genetic analysis of p38 MAP kinases in myogenesis: fundamental role of p38alpha in abrogating myoblast proliferation. EMBO J. 26, 1245–1256.

Pollack, A., Bae, K., Khor, L.Y., Al-Saleem, T., Hammond, M.E., Venkatesan, V., Byhardt, R.W., Asbell, S.O., Shipley, W.U., and Sandler, H.M. (2009). The importance of protein kinase A in prostate cancer: relationship to patient outcome in Radiation Therapy Oncology Group trial 92-02. Clin. Cancer Res. 15, 5478–5484.

Rommel, C., Clarke, B.A., Zimmermann, S., Nuñez, L., Rossman, R., Reid, K., Moelling, K., Yancopoulos, G.D., and Glass, D.J. (1999). Differentiation stage-specific inhibition of the Raf-MEK-ERK pathway by Akt. Science 286, 1738–1741.

Rothman, D.M., Shults, M.D., and Imperiali, B. (2005). Chemical approaches for investigating phosphorylation in signal transduction networks. Trends Cell Biol. 15, 502–510.

Sato, M., Kawai, Y., and Umezawa, Y. (2007). Genetically encoded fluorescent indicators to visualize protein phosphorylation by extracellular signal-regulated kinase in single living cells. Anal. Chem. 79, 2570–2575.

Shults, M.D., and Imperiali, B. (2003). Versatile fluorescence probes of protein kinase activity. J. Am. Chem. Soc. 125, 14248–14249.

Shults, M.D., Janes, K.A., Lauffenburger, D.A., and Imperiali, B. (2005). A multiplexed homogeneous fluorescence-based assay for protein kinase activity in cell lysates. Nat. Methods 2, 277–283.

Stains, C.I., Luković, E., and Imperiali, B. (2011). A p38α-selective chemosensor for use in unfractionated cell lysates. ACS Chem. Biol. 6, 101–105.

Tagawa, M., Ueyama, T., Ogata, T., Takehara, N., Nakajima, N., Isodono, K., Asada, S., Takahashi, T., Matsubara, H., and Oh, H. (2008). MURC, a muscle-restricted coiled-coil protein, is involved in the regulation of skeletal myogenesis. Am. J. Physiol. Cell Physiol. 295, C490–C498.

Tomczak, K.K., Marinescu, V.D., Ramoni, M.F., Sanoudou, D., Montanaro, F., Han, M., Kunkel, L.M., Kohane, I.S., and Beggs, A.H. (2004). Expression profiling and identification of novel genes involved in myogenic differentiation. FASEB J. 18, 403–405.

Wang, H.X., Xu, Q., Xiao, F., Jiang, Y., and Wu, Z.G. (2008). Involvement of the p38 mitogen-activated protein kinase alpha, beta, and gamma isoforms in myogenic differentiation. Mol. Biol. Cell *19*, 1519–1528.

Wang, Q., Cahill, S.M., Blumenstein, M., and Lawrence, D.S. (2006). Self-reporting fluorescent substrates of protein tyrosine kinases. J. Am. Chem. Soc. *128*, 1808–1809.

Wang, Q., Zimmerman, E.I., Toutchkine, A., Martin, T.D., Graves, L.M., and Lawrence, D.S. (2010). Multicolor monitoring of dysregulated protein kinases in chronic myelogenous leukemia. ACS Chem. Biol. *5*, 887–895.

Xiao, K., Sun, J., Kim, J., Rajagopal, S., Zhai, B., Villén, J., Haas, W., Kovacs, J.J., Shukla, A.K., Hara, M.R., et al. (2010). Global phosphorylation analysis of β-arrestin-mediated signaling downstream of a seven transmembrane receptor (7TMR). Proc. Natl. Acad. Sci. USA *107*, 15299–15304.